

Supplementary Information

Morphology-Dependent Fluorescence of Europium-Doped Cerium Oxide Nanomaterials

Anne E. D'Achille,^a Robert M. Wallace,^b Jeffery L. Coffer*^a

^aDepartment of Chemistry and Biochemistry, Texas Christian University, Fort Worth TX 76129

^bDepartment of Materials Science, University of Texas-Dallas, Richardson, TX 75080

List of contents

Equation S1. Working Definition of theoretical Eu³⁺ doping percentage.

Figure S1. Diagram of electrospinning apparatus.

Figure S2. Representative SEM images of (a) unannealed 8% Eu-CeO₂/PVP nanowires, and (b) annealed 8% Eu-CeO₂ nanowires.

Figure S3. Histograms of 8%-Eu-CeO₂ (a) nanorod length, (b) nanorod width, (c) annealed nanorod length (d) annealed nanorod width, (e) nanowire diameters, and (f) nanocube edge length.

Equation S2. Scherrer formula and associated definitions.

Figure S4. XRD spectra of 8 %Eu-CeO₂ nanomaterials.

Table S1. Atomic percentage of Eu in CeO₂ nanorods, nanowires, nanocubes, and annealed nanorods, calculated excluding oxygen as determined by EDS analysis.

Table S2. Atomic percentage of europium, cerium, and oxygen in CeO₂ nanorods, nanowires, nanocubes, and annealed nanorods as determined by EDS analysis.

Table S3. Binding energies and areas from fitted Ce 3d XPS spectra for 8% Eu-CeO₂ nanomaterials and undoped CeO₂ nanorods.

Table S4. Binding energies and integrated areas from fitted O 1s XPS spectra for 8%-Eu-CeO₂ nanomaterials and undoped CeO₂ nanorods.

Figure S5. XPS spectra of Ce 3d (a) CeO₂ nanorod, (b) 8% Eu-CeO₂ nanocube, (c) 8% Eu-CeO₂ nanowires, and O 1s of (d) CeO₂ nanorods, (e) 8% Eu-CeO₂ nanocubes, and (f) 8% Eu-CeO₂ nanowires.

Figure S6. FT IR spectra of cerium oxide nanorods before and after annealing, showing significant loss of hydroxyl stretching mode intensity ~ 3200 cm⁻¹ upon heating the sample.

Figure S7. Normalized absorbance spectra of 8 at% Eu-CeO₂ nanowires (75 µg/mL), nanorods (260 µg/mL), nanocubes (112 µg/mL), and annealed nanorods (188 µg/mL).

Figure S8. UV-Vis absorbance spectra with varying Eu³⁺ concentration for CeO₂ (a) nanowires, (b) nanorods, (c) nanocubes, and (d) annealed nanorods.

Figure S9. Excitation spectrum for nanocubes measuring emission at 590 nm.

Table S5. Asymmetry ratio of 8% Eu-CeO₂ nanorods with increasing annealing temperature with excitation at 375 nm.

Equation S1. Working Definition of theoretical Eu³⁺ doping percentage.

The theoretical Eu³⁺ concentration with regard to atomic percentage within each material ranges from 0% to 18% Eu³⁺, as calculated by Equation 1, and based on experimental reactant concentrations:

$$\%Eu = mM\ Eu^{3+} / (mM\ Eu^{3+} + mM\ Ce^{3+}) \quad (\text{S1})$$

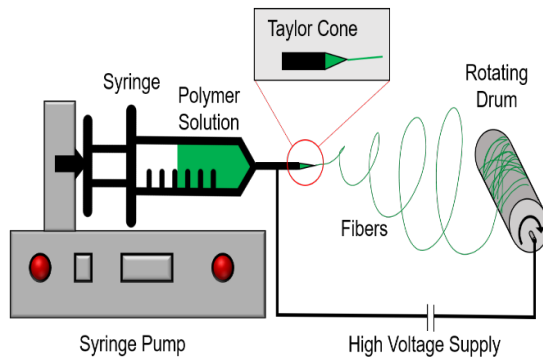


Figure S1. Diagram of electrospinning apparatus.

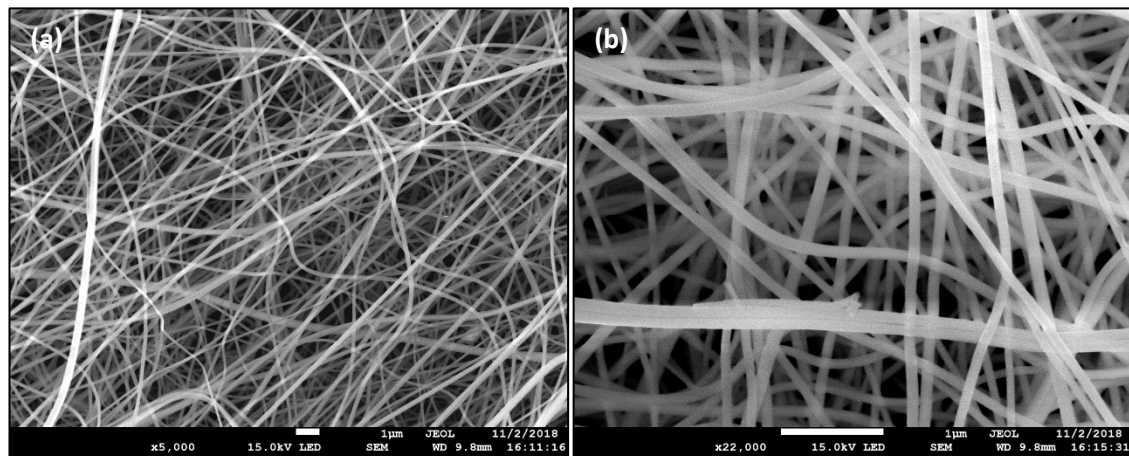


Figure S2. Representative SEM images of (a) unannealed 8% Eu-CeO₂/PVP nanowires, and (b) annealed 8% Eu-CeO₂ nanowires.

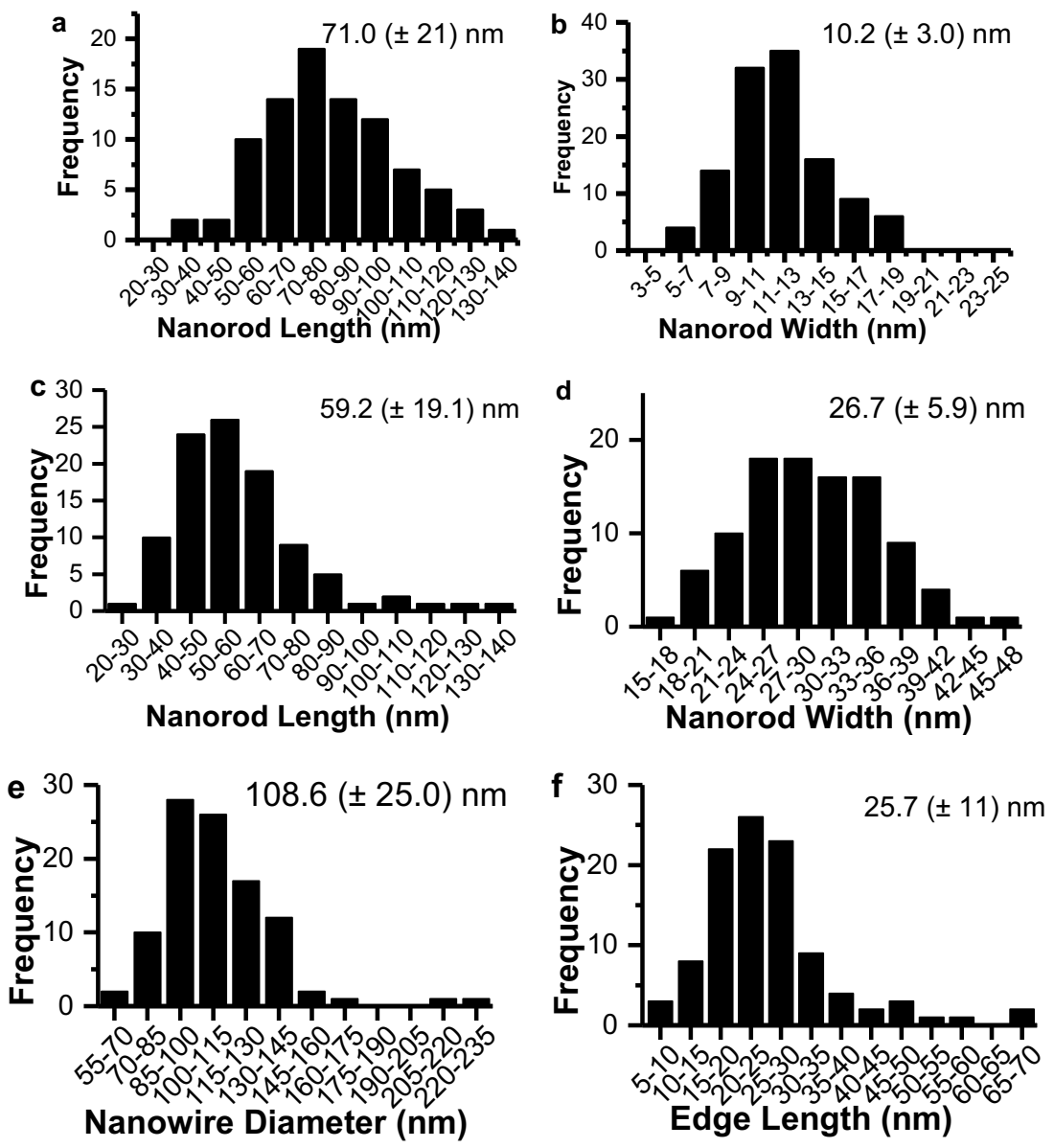


Figure S3. Histograms of 8%-Eu-CeO₂ (a) nanorods length, (b) nanorods width, (c) annealed nanorods length (d) annealed nanorods width, (e) nanowire diameters, and (f) nanocube edge length.

Equation S2. Scherrer formula and associated definitions. Crystalline domain sizes are estimated by use of the Scherrer equation (Equation S2). Here τ is the crystalline domain size in nm, K is the shape constant approximated to be 0.94, λ is the wavelength of the incident x-rays (1.54178 Å for Cu K_a), β is the full-width half-max of the CeO₂ (111) peak at 31° and, θ is the Bragg angle, or $\frac{1}{2}$ the 2θ x-ray angle.

$$\tau = \frac{K\lambda}{\beta \cos(\theta)} \quad (\text{S2})$$

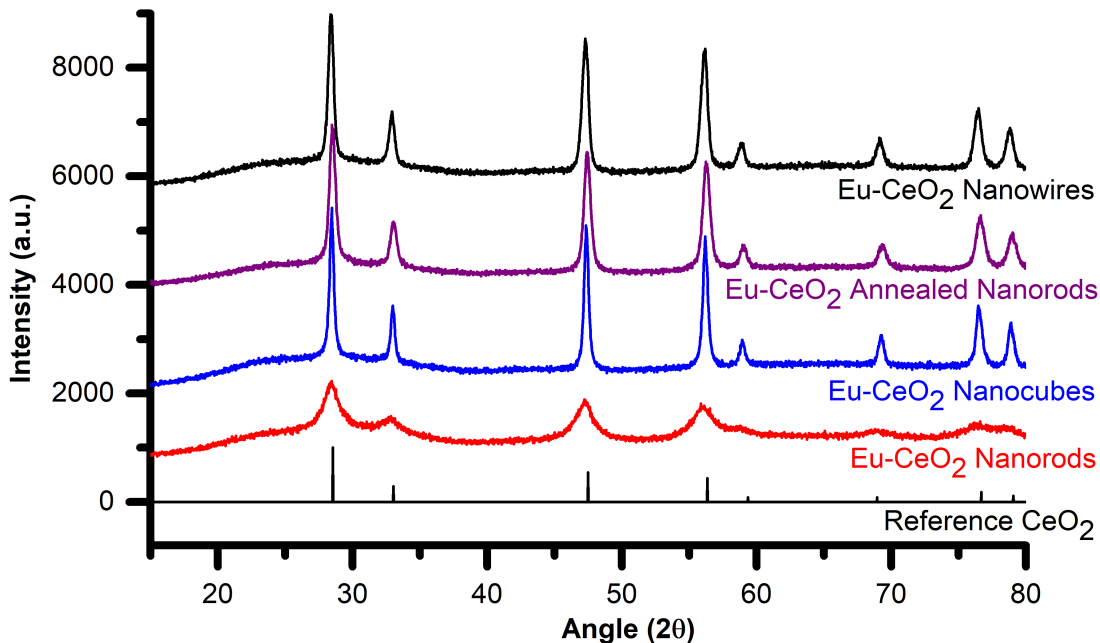


Figure S4. XRD spectra of 8 %Eu-CeO₂ nanomaterials.

Table S1. Atomic percentage of Eu³⁺ in CeO₂ nanorods, nanowires, nanocubes, and annealed nanorods, calculated without consideration to oxygen as determined by EDS analysis.

	Undoped	2% Eu	8% Eu	15%
Nanowire	0.0 ± 0.0	2.4 ± 0.7	9.7 ± 1.7	16.2 ± 0.5
Nanorod	0.2 ± 0.2	3.1 ± 1.0	7.9 ± 1.7	15.6 ± 0.7
Annealed Nanorod	1.1 ± 0.9	3.1 ± 0.9	7.0 ± 0.9	15.7 ± 0.4
Nanocube	0.2 ± 0.2	2.9 ± 1.0	6.8 ± 0.9	11.7 ± 0.3

Table S2. Atomic percentage of europium, cerium, and oxygen in CeO₂ nanorods, nanowires, nanocubes, and annealed nanorods as determined by EDS analysis.

		0% Eu-CeO ₂	2% Eu-CeO ₂	8% Eu-CeO ₂	15% Eu-CeO ₂
Nanowire	% O	52.5 ± 6.8	51.4 ± 0.9	53.1 ± 4.3	51.1 ± 2.3
	% Ce	47.1 ± 4.8	46.0 ± 2.4	42.3 ± 3.8	41.1 ± 2.2
	% Eu	0.0 ± 0.0	1.15 ± 0.4	4.6 ± 0.9	7.9 ± 0.1
Nanorod	% O	62.7 ± 7.2	68.6 ± 8.0	62.1 ± 5.5	60.5 ± 1.3
	% Ce	37.2 ± 7.2	30.5 ± 8.0	34.2 ± 4.6	32.2 ± 1.9
	% Eu	0.1 ± 0.1	0.9 ± 0.1	3.7 ± 0.9	7.3 ± 1.9
Annealed Nanorod	% O	65.6 ± 6.7	57.8 ± 0.9	60.2 ± 1.9	56.3 ± 3.8
	% Ce	32.1 ± 6.9	40.9 ± 1.3	37.0 ± 2.1	36.7 ± 3.4
	% Eu	0.33 ± 0.3	1.3 ± 0.4	2.8 ± 0.4	6.9 ± 0.4
Nanocube	% O	53.5 ± 0.9	51.9 ± 1.6	54.3 ± 3.6	55.8 ± 1.1
	% Ce	46.4 ± 0.9	46.7 ± 1.2	42.6 ± 3.7	39.0 ± 1.1
	% Eu	0.1 ± 0.1	1.4 ± 0.6	3.1 ± 0.2	5.2 ± 0.1

Table S3. Binding energies and areas from fitted Ce 3d XPS spectra for 8% Eu-CeO₂ nanomaterials and undoped CeO₂ nanorods.

	<i>u</i>	<i>u'</i>	<i>u''</i>	<i>u'''</i>	<i>v</i>	<i>v'</i>	<i>v''</i>	<i>v'''</i>
CeO₂ Nanorod								
Binding Energy (eV)	881.89	884.87	888.27	897.89	900.53	903.45	906.73	916.33
Integrated Area	8259.7	4762.6	3694.8	5993.1	5153.2	2168.8	2296.6	4336.1
Eu-CeO₂ Nanorod								
Binding Energy (eV)	881.86	884.69	888.20	898.0	900.61	903.20	906.70	916.37
Integrated Area	6423.7	4434.9	3933.5	5752.9	4034.0	2161.2	2336.1	3710.6
Eu-CeO₂ Annealed Rod								
Binding Energy (eV)	881.95	884.92	888.35	897.74	900.53	903.45	906.97	916.17
Integrated Area	5561.9	1863.9	3506.	5379.1	3551.2	938.2	2143.31	3898.86
Eu-CeO₂ Nanowire								
Binding Energy (eV)	881.9	884.6	888.2	897.9	900.4	902.4	906.9	916.1
Integrated Area	26655	4786	4835	16583	8056	1108	1442	8279
Eu-CeO₂ Nanocube								
Binding Energy (eV)	882.00	883.50	888.04	898.10	901.03	903.89	907.11	916.46
Integrated Area	2287.95	1838.26	1834.6	3172.9	1720.34	293.87	902.894	2021.89

Table S4. Binding energies and integrated areas from fitted O 1s XPS spectra for 8%-Eu-CeO₂ nanomaterials and undoped CeO₂ nanorods.

	O _α		O _β	
	Binding Energy (eV)	Integrated Area	Binding Energy	Integrated Area
CeO₂ Nanorod	528.95	5017.1	531.40	1055.4
Eu-CeO₂ Nanorod	528.99	4282.6	531.39	1478.6
Eu-CeO₂ Annealed Nanorod	528.69	4454.6	531.32	1234.8
Eu-CeO₂ Nanowire	~529.3	15639.2	~531.99	2460.4
Eu-CeO₂ Nanocube	529.16	4657.9	532.04	500.4

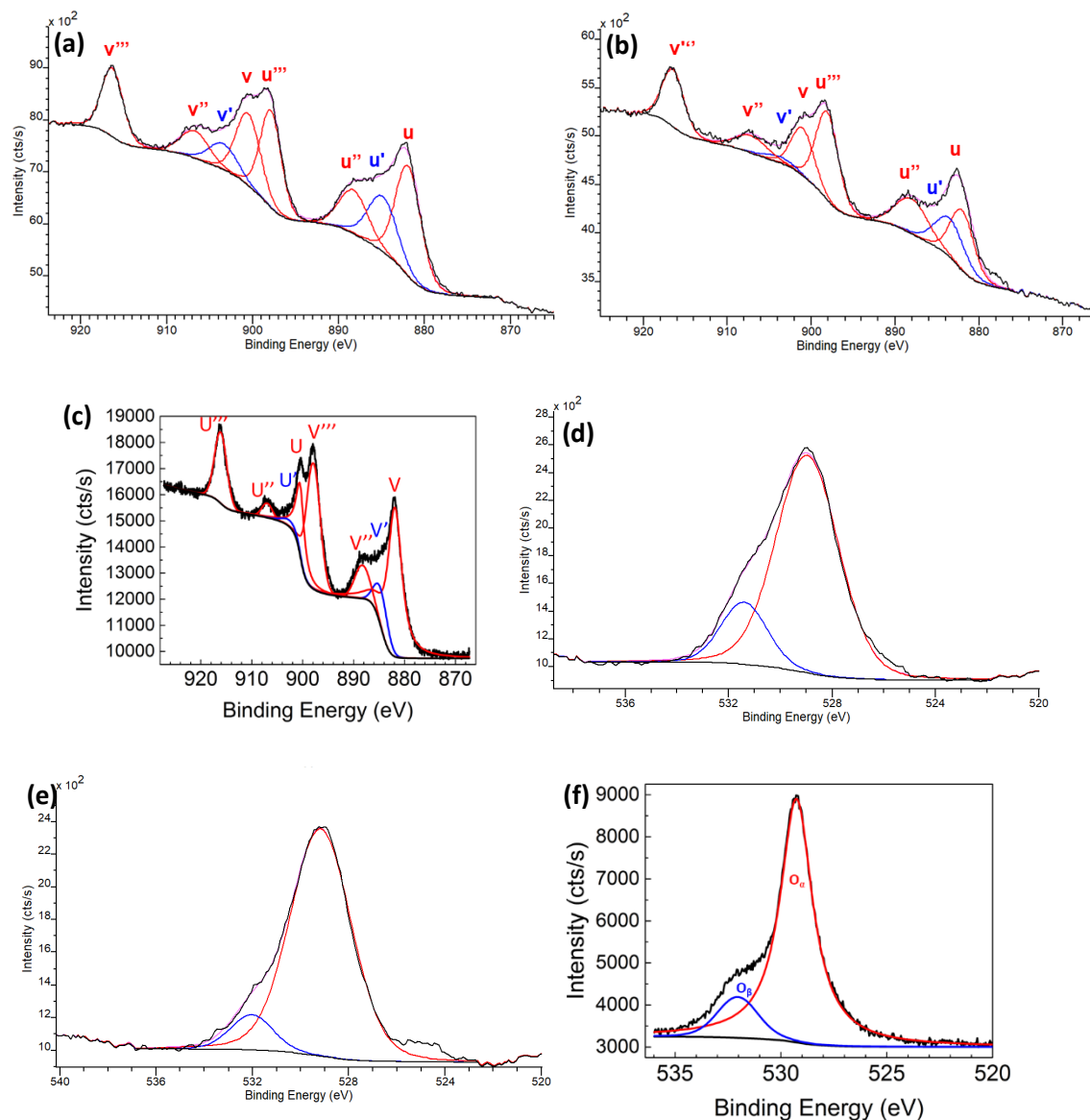


Figure S5. XPS spectra of Ce 3d (a) CeO₂ nanorod, (b) 8% Eu-CeO₂ nanocubes, (c) 8% Eu-CeO₂ nanowires, and O 1s (d) CeO₂ nanorods, (e) 8% Eu-CeO₂ nanocubes, and (f) 8% Eu-CeO₂ nanowires.

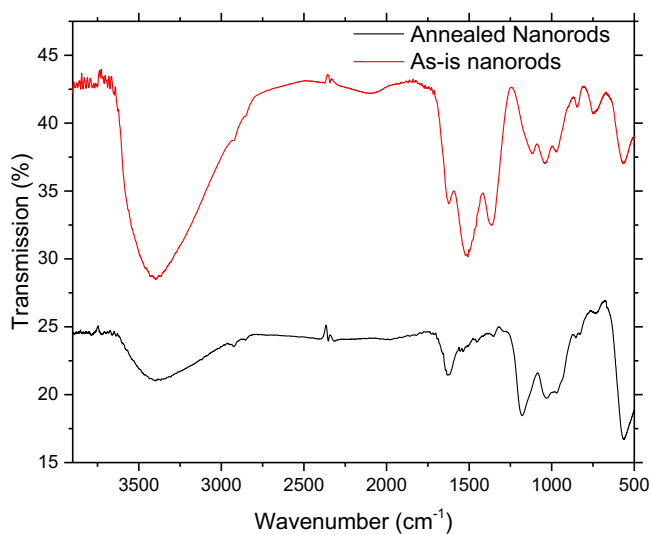


Figure S6. FT IR spectra of cerium oxide nanorods before and after annealing at 600°C.

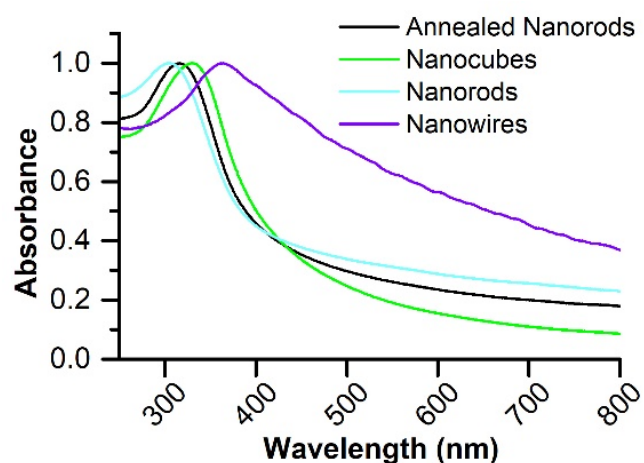


Figure S7. Normalized absorbance spectra of 8 at% Eu-CeO₂ nanowires (75 µg/mL), nanorods (260 µg/mL), nanocubes (112 µg/mL), and annealed nanorods (188 µg/mL).

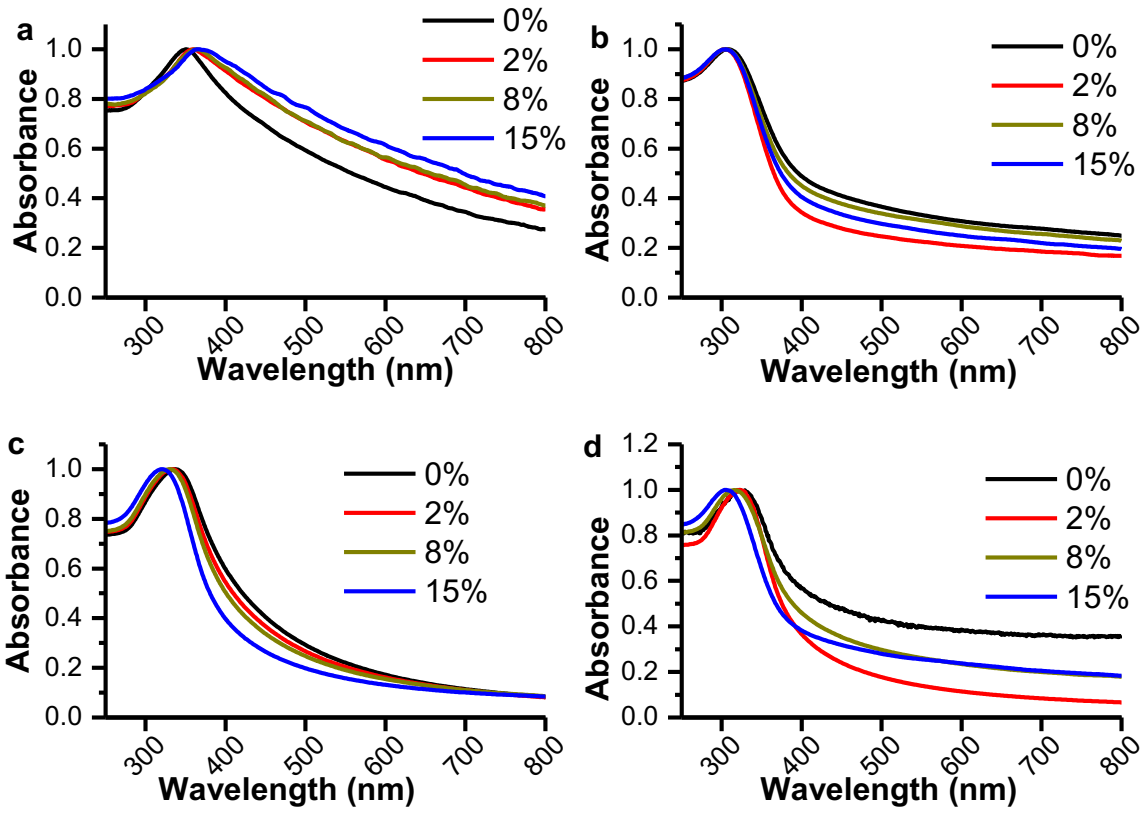


Figure S8. UV-Vis absorbance with varying Eu³⁺ concentration for CeO₂ (a) nanowires, (b) nanorods, (c) nanocubes, and (d) annealed nanorods.

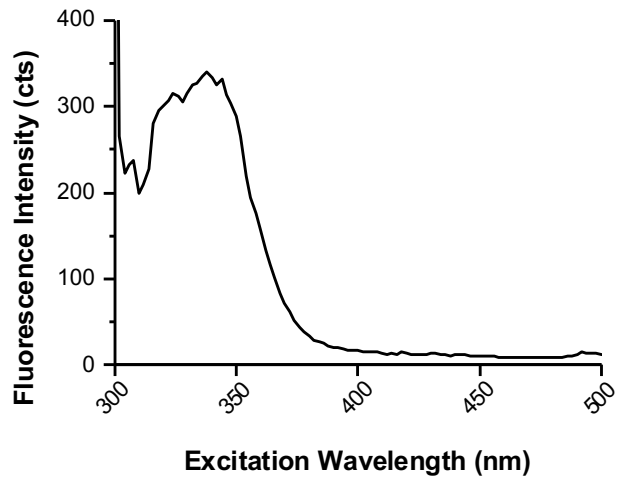


Figure S9. Excitation spectrum for nanocubes measuring emission at 590 nm.

Table S5. Asymmetry ratio of 8% Eu-CeO₂ nanorods with increasing annealing temperature with excitation at 375 nm.

Annealing Temperature	Unannealed	400 °C	500 °C	600 °C	700 °C	800 °C
Asymmetry Ratio	1.99	2.49	2.29	2.32	2.23	2.19